conclusion that the high conductances indicate complete dissociation.

The continuous change in the internal structure of electrolyte solutions with increasing concentration toward that of an ionic melt is represented by the solubility curve for halite as a function of temperature, which is continuous with the melting curve for the salt at pressures >400 bars (*19*). It thus appears that the structure of a saturated electrolyte solution at supercritical pressures and temperatures, where $\epsilon \lesssim 15$, may consist of a single macroscopic cluster, a megacluster, of essentially all of the solute species in solution. Such a cluster represents the culmination of the sequential formation of successively higher order clusters with increasing concentration as the solution approaches the state of a molten salt (Fig. 3).

Due to the paucity of experimental data, the calculations summarized above should be regarded as yielding provisional estimates only. Nevertheless, it appears that speciation in concentrated supercritical aqueous single-electrolyte solutions may be more complex than was generally thought to be the case. Depending on the temperature and pressure, speciation in these solutions may be dominated by successively higher order clusters at progressively higher solute concentrations. The presence of these polyatomic clusters may profoundly affect the thermodynamic properties of concentrated electrolyte solutions, as well as the solubilities of minerals in these solutions at supercritical pressures and temperatures.

REFERENCES AND NOTES

1. E. U. Franck, *Phys. Chem.* **8**, 92 (1956); G. Ritzert and E. U. Franck, *Bunsen. Phys. Chem.* **72**, 798 (1968); A. S. Quist and W. L. Marshall, *J. Phys. Chem.* **72**, 648 (1968); *ibid.*, p. 1545; L. A. Dunn and W. L. Marshall, *ibid.* **73**, 723 (1969); J. D. Frantz and W. L. Marshall, *Am. J. Sci.* **282**, 1666 (1982).
2. D. A. Sverjensky, in *Thermodynamic Modeling of Geologic Materials: Minerals, Fluids and Melts*, I. S. E. Carmichael and H. P. Eugster, Eds., vol. 17 of *Reviews in Mineralogy* (Mineralogical Society of America, Washington, DC, 1987), pp. 177–209; H. P. Eugster and L. Baumgartner, *ibid.*, pp. 367–404.
3. H. S. Harned and B. B. Owen, *The Physical Chemistry of Electrolyte Solutions* (Reinhold, New York, 1958); H. C. Helgeson and D. H. Kirkham, *Am. J. Sci.* **276**, 97 (1976); J. V. Walther and J. Schott, *Nature* **322**, 635 (1988); R. W. Gurney, *Ionic Processes in Solution* (Dover, New York, 1962); F. Franks, in *Water, A Comprehensive Treatise*, F. Franks, Ed. (Plenum, New York, 1973), vol. 2, pp. 1–54; P. V. Brady and J. V. Walther, *Geochim. Cosmochim. Acta* **54**, 1555 (1990); J.-L. Dandurand and J. Schott, *J. Phys. Chem.* **96**, 7770 (1992).
4. J. W. Johnson and D. Norton, *Am. J. Sci.* **291**, 541 (1991).
5. R. M. Fuoss and C. A. Kraus, *J. Am. Chem. Soc.* **55**, 3614 (1933); H. S. Young and C. A. Kraus, *ibid.* **73**, 4732 (1951); D. T. Copenhafer and C. A. Kraus, *ibid.*, p. 4557; M. Hojo, A. Tanio, Y. Miyauchi, Y. Imai, *Chem. Lett.* **1991**, 1827 (1991).
6. E. H. Oelkers and H. C. Helgeson, *Geochim. Cosmochim. Acta* **55**, 1235 (1991).
7. ——— *ibid.* **54**, 727 (1990).
8. K. S. Pitzer and D. R. Schreiber, *Mol. Phys.* **60**, 1067 (1987).
9. E. H. Oelkers and H. C. Helgeson, *Geochim. Cosmochim. Acta* **57**, 2673 (1993).
10. Values of $\hat{a}_j$ and α_j for supercritical NaCl solutions were calculated by minimizing the Gibbs free energy of the solution by using apparent standard partial molal Gibbs free energies of formation ($\Delta\overline{G}°$) of the solute species computed from logarithms of the overall dissociation constants (log β) of diatomic neutral ion pairs and polyatomic clusters (*9*) and values of $\Delta\overline{G}°$ for monatomic ions were calculated from the revised HKF equations of state (*11*). The standard state used in the calculations consisted of unit activity of the solute in a hypothetical 1 *m* solution referenced to infinite dilution at any pressure and temperature. The values of log β for triple, quadruple, quintuple, and sextuple clusters were generated from the results of Monte Carlo calculations (*12*) for the restricted primitive model by replacing the arbitrary hard sphere diameter (δ_H) used in these calculations with temperature- and pressure-dependent values obtained by regression of the logarithms of experimental dissociation constants (*1, 9, 13*) for diatomic neutral ion pairs (log *K*) with the molal analog of Gillan's (*12*) equation 9. This procedure renders the results of the Monte Carlo calculations consistent with the conductance data from which the values of log *K* were generated (*13*). The values of log β for triple ions computed in this manner are in general agreement with those predicted from electrostatic theory. The speciation calculations were carried out assuming the degrees of formation of septuple and larger clusters to be negligible at NaCl concentrations <1 *m*. Activity coefficients for charged and neutral aqueous species computed from the Hückel (*7, 14*) and Setchénow (*6, 15*) equations, respectively, were used in the calculations to account for cluster-cluster and cluster-solvent interactions with increasing solute concentration. The activity coefficients of the charged and neutral clusters were assumed in a first approximation to be equal to those of NaCl and $NaCl^0$, respectively.
11. E. L. Shock, E. H. Oelkers, J. W. Johnson, D. A. Sverjensky, H. C. Helgeson, *J. Chem. Soc. Faraday Trans.* **88**, 803 (1992); J. W. Johnson, E. H. Oelkers, H. C. Helgeson, *Comput. Geosci.*, **18**, 899 (1992).
12. M. J. Gillan, *Mol. Phys.* **49**, 421 (1983).
13. E. H. Oelkers and H. C. Helgeson, *J. Phys. Chem.* **92**, 1631 (1988).
14. H. C. Helgeson, D. H. Kirkham, G. C. Flowers, *Am. J. Sci.* **281**, 1249 (1981).
15. M. Setchénow, *Ann. Chim. Phys.* **25**, 225 (1892).
16. C. A. Kraus, *J. Phys. Chem.* **58**, 673 (1954); *ibid.* **60**, 129 (1956).
17. V. M. Valyashko, *Bunsen Phys. Chem.* **81**, 388 (1977).
18. J. U. Hwang, H. D. Ludemann, D. Hartmann, *High Pressures High Temperatures* **2**, 651 (1970).
19. T. S. Bowers and H. C. Helgeson, *Geochim. Cosmochim. Acta* **47**, 1247 (1983).

20. This research was supported by the National Science Foundation (NSF grant EAR-8606052), the Department of Energy (DOE grant DE-FG03-85ER-13419), and the Committee on Research at the University of California. We thank B. Ransom, W. Murphy, J. Johnson, D. Sverjensky, V. Pokrovskii, E. Shock, J. Schott, C. Monnin, and J. Amend for discussions and assistance; J. Bossart for word processing; R. Arington, K. Hwang, and Christine Owens for drafting the figures; J. Hampel and P. Gennaro for photographic assistance; and the reviewers for helpful suggestions and constructive criticism.

12 March 1993; accepted 16 June 1993

Protein Catalysis of the Retinal Subpicosecond Photoisomerization in the Primary Process of Bacteriorhodopsin Photosynthesis

Li Song, M. A. El-Sayed,* J. K. Lanyi

The rate of retinal photoisomerization in wild-type bacteriorhodopsin (wt bR) is compared with that in a number of mutants in which a positively charged (Arg^{82}), a negatively charged (Asp^{85} or Asp^{212}), or neutral hydrogen bonding (Asp^{115} or Tyr^{185}) amino acid residue known to be functionally important within the retinal cavity is replaced by a neutral, non–hydrogen bonding one. Only the replacements of the charged residues reduced the photoisomerization rate of the 13-*cis* and *all-trans* isomers present in these mutants by factors of ~1/4 and ~1/20, respectively. Retinal photo- and thermal isomerization catalysis and selectivity in wt bR by charged residues is discussed in terms of the known protein structure, the valence-bond wave functions of the ground and excited state of the retinal, and the electrostatic stabilization interactions within the retinal cavity.

Bacteriorhodopsin (bR), the other natural photosynthetic system besides chlorophyll, is a light-transducing protein present in the purple membrane of *Halobacterium halobium*. Since its discovery by Oesterhelt and Stoeckenius (*1*) in 1971 and the demonstration of its role in adenosine triphosphate (ATP) synthesis by Racker and Stoeckenius (*2*), numerous studies have been carried out to unravel its structure and the mechanism of its function (*3*). Not only is bR an important natural solar energy converter, but it is also becoming a potentially important biomaterial for photonic applications (*4, 5*) with uses in holographic recording, as ultrafast diodes, in neural networks, associative memory, and it might possibly be used as the "eyes of robots" (*5*).

L. Song and M. A. El-Sayed, Department of Chemistry and Biochemistry, University of California, Los Angeles, Los Angeles, CA 90024–1569.
J. K. Lanyi, Department of Physiology and Biophysics, University of California, Irvine, Irvine, CA 92717.

*To whom correspondence should be addressed.

The free energy resulting from the storage of the absorbed photon with energy $h\nu$ by the retinal drives the system through the following photochemical cycle and pumps protons against an electrochemical gradient:

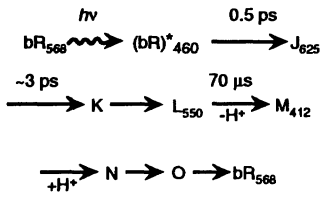

The structure of the retinal pocket has been determined by a number of techniques. Neutron diffraction has shown that the protonated Schiff base is located midway between the C and G helices (6) and is ~15 Å from the extracellular membrane surface (7). The ionone ring is only 9 Å away from this surface, thus in agreement with the linear dichroism results (8) that the retinal long axis is oriented toward the cell exterior. From site-directed mutagenesis (SDM) (9) together with Fourier transform infrared FTIR (10, 11) spectroscopic studies and electron diffraction results (12), it was concluded that Arg^{82}, Tyr^{185}, Asp^{85}, and Asp^{212} form the environment around the Schiff base region. The important Schiff base counterion is thought to be either Asp^{85} or Asp^{212} (8, 13). Both are in the ionized form (11) in bR_{568}. Mathies *et al.* (14), who energy-minimized the Henderson *et al.* structure (12), concluded that Asp^{212} is an important counterion that is weakly hydrogen bonded to the protonated Schiff base in order to maximize hydrogen bonding to both Tyr^{185} and the indole nitrogen of Trp^{86}.

Two different theoretical molecular dynamics (MD) models (15) have been proposed. In one model, the primary product of the photoisomerization process is the 13-*cis*, and in the other one the 13,14-di*cis* is proposed. The effect of charge stabilization by charged protein groups on the potential surface of the retinal chromophore has been previously discussed (16).

Time-resolved optical spectroscopy has shown changes in the visible absorption spectrum on a subpicosecond time scale (17–19). The results of the most recent optical studies by Mathies *et al.* (18) with 6-fs laser pulses suggest that molecules in the excited state relax in 200 fs from the Frank-Condon configuration resulting from the absorption process, and then decay in 500 fs to form J_{625}. The structure of the intermediates during the bR photocycle has been identified by using time-resolved Raman spectroscopy (20). More recent experiments with subpicosecond time-resolved Raman techniques have shown (21) that the first intermediate of the bR photocycle is indeed an isomer of bR_{568}.

A photoisomerization process in 500 fs in a molecule of the size of the retinal within a tight protein cavity such as that of the bR opsin seems to be unusually rapid. This observation suggests that the amino acid residues of the protein in the retinal cavity are arranged in such a manner as to render the photoisomerization of the retinal around the C13–C14 bond barrierless. In order to understand the origin of this catalysis, we have determined the retinal photoisomerization rate for different bR mutants in which individual, functionally important, charged and neutral amino acid residues within the retinal cavity are replaced by neutral ones. In the mutants used in this study, the negatively charged residues Asp^{85} and Asp^{212}, the positively charged residue Arg^{82}, and hydrogen-bonding neutral residues Asp^{115} and Tyr^{185} were replaced individually by non–hydrogen-bonding neutral residues. The results suggest that the charged residues such as Asp^{85}, Asp^{212}, and Arg^{82} are the only residues that catalyze the photoisomerization process. A possible molecular mechanism for the catalysis and the selectivity of the retinal photo- and thermal isomerization process by charged residues is proposed.

In our experiment, a pump-probe transient optical absorption setup in the subpicosecond time scale was used (22). The SDM procedure was described previously (23, 24). The purified mutant bR suspensions in deionized water were stored in 2-mm quartz cells (with an optical density of 0.3 to 0.5). All of the experiments were performed at room temperature (~20°C). In order to change the pH of the sample over a wide range without causing sample aggregation, some mutants were studied in polyacrylamide gels. This difference had little effect on the observed decay of wt bR and no detectable change was observed for the other mutants.

The transient absorption for wt bR and some of its mutants were studied as function of the delay time between the pump pulse and the probe pulse. At the probe wavelength of 489 nm, the predominant absorption of the wt bR is assigned to the excited singlet state absorption (19). Therefore the decay of the transient signal is due to the decay of the population in the excited state resulting from the retinal isomerization process to form the J_{625} intermediate.

The observed decay curves for the retinal excited state of wt bR and some of its mutants are shown in Fig. 1 and a summary of the decay parameters obtained from the best fit to one or two exponential decays convoluted with a laser pulse function are given in Table 1. The important results and conclusions are:

1) Only charged residue substitution reduces the photoisomerization rates. Substitution of neutral residues (Tyr^{185} and Asp^{115}) did not significantly affect the photoisomerization rate (see the dotted decay curve in Fig. 1E for Tyr^{185}).

2) The replacement of Asp^{85} by a neutral amino acid (Asn) gives rise to two decay components of 2- and 10-ps lifetimes. Both are much longer than that observed in wt bR (0.5 ps). These two components in D85N (25) closely resemble those observed for the deionized blue

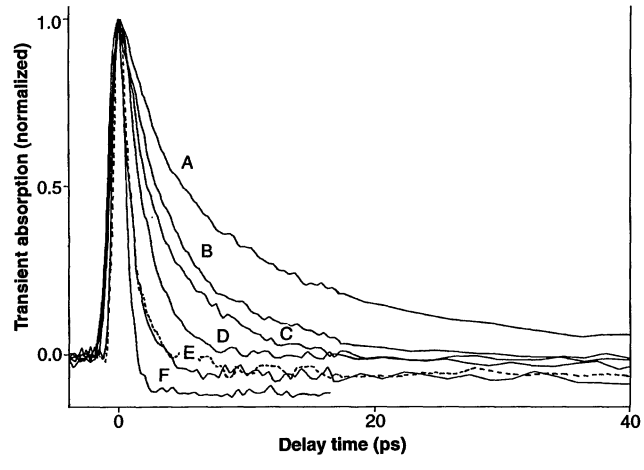

Fig. 1. Effect of site-selected replacement of functionally important charged amino acid residues within the retinal pocket of bR on the rate of photoisomerization. The curves shown are the decays of the retinal excited-state absorption due to the photoisomerization as monitored by the pump-probe technique on subpicosecond time scale. The curves in the figure from top to bottom are: (**A**) D85N at pH 5.8 in 0.1 M Na_2SO_4 solution; (**B**) R82Q at pH 4.4 in polyacrylamide gel; (**C**) D212N in pH 5 potassium phosphate buffer solution; (**D**) D212N in pH 10 buffer solution; (**E**) solid curve, R82Q in pH 9.6 buffer solution; dotted curve, Y185F in pH 5.8 buffer solution; and (**F**) wt bR in pH 5.8 buffer solution. These charged residue replacements slow down photoisomerization (elongate the excited-state decay), suggesting their involvement in the protein photocatalysis of the primary process of bR photosynthesis (replacement of neutral hydrogen bonding residues within the cavity did not affect the rate of photoisomerization, see Table 1).

bR and assigned by Kobayashi *et al.* (26) to the 13-*cis* isomer (short lifetime) and *all-trans* (long lifetime) isomer. If the same assignment is made in D85N, one concludes that the rate of isomerization of the *all-trans* retinal is reduced by a factor of 20 upon the replacement of the COO^- group of Asp^{85} by a neutral group (Asn).

3) Upon replacing Arg^{82} by a neutral residue (for example, in R82Q), the isomerization rate is found to decrease as shown in Fig. 1B by the observed increase in the excited-state lifetime of the retinal at pH 4.4. The slow component in R82Q is found to have a photoisomerization rate that is 14 times slower than that in wt bR.

It is believed (*13*) that Arg^{82+} decreases the pK_a (acidity constant) of Asp^{85} in the wt bR to keep its carboxylic group in its ionized form at physiological pH. This is consistent with the observation that the pK_a of Asp^{85} is increased from below 3 in the wt bR to ~7.5 in R82Q (*27*). At pH 9.6, the carboxylic group of Asp^{85} in R82Q is deionized, and the photoisomerization is thus expected to be catalyzed. Indeed, the observed rate of retinal photoisomerization in R82Q at pH 9.6 (concluded from its excited-state decay in Fig. 1E) was not significantly different from that observed for wt bR at the same pH.

4) The replacement of Asp^{212} by a neutral residue is also found to increase the retinal excited-state lifetime. This mutant is purple at low pH (for example, pH = 5) but blue at high pH (such as pH = 10), opposite to that observed for wt bR (*24*). The excited-state decay of retinal in the purple form of D212N was 2.0 and 6.0 ps for the two isomers at pH 5 but only one decay component of 2.0 ps was found at pH 10. Under both pH conditions, the isomerization time was longer than in wt bR, but for one isomer the purple form has longer isomerization time. This suggests that the observed retinal absorption maximum and its rate of photoisomerization are not correlated. This is further illustrated in Table 1, in which the decay times, the relative amplitude for both decay components, as well as the absorption maximum of each sample studied are given. This lack of correlation is expected. The photoisomerization rate depends on the potential surface around the retinal in the excited state, whereas the absorption maximum depends on the energy difference between the excited-state and ground-state potential energy surfaces at the ground-state equilibrium configuration. The difference in the retinal excited-state lifetimes of D212N at the two pH values is likely due to changes in the retinal-protein conformation as a result of changes in the acid-base equilibrium of a nearby residue or residues.

5) The rate of retinal isomerization in D115N and Y185F is similar to that of wt bR under similar conditions, which suggests that neutral residues like Asp^{115} and Tyr^{185} do not affect the rate of isomerization in wt bR.

The above results show that the negative charge of Asp^{85} and Asp^{212} as well as the positive charge of Arg^{82} have strong catalytic function in the retinal photoisomerization process in wt bR. The catalysis due to Arg^{82+} can be traced to its function in insuring that the COOH group of Asp^{85} is in its ionized form at physiological pH, which is required for the photoisomerization catalysis. In the absence of Asp^{212}, the rate of the retinal photoisomerization is found to be faster at higher pH, suggesting the importance of another residue that is deprotonated at this pH (pH = 10).

In both of the previous 13-*cis* and 13,14-di*cis* MD models (*15*), the intramolecular barrier to the retinal isomerization is an important factor in determining the reaction rate. This barrier is determined by the bond order of the bonds around which isomerization takes place. As its value increases above unity in the ground or in the excited state, the rate of the retinal thermal or photoisomerization, respectively, is expected to diminish. Thus the structure of the retinal that is undergoing the isomerization process is most important. Below, we use a valence bond resonance approach to show how the structures of the ground and the excited state of retinal can be determined by the stabilization of the positive charge either on the nitrogen atom or on the carbon atoms by the COO^- groups of Asp^{85} and Asp^{212}.

The ground electronic state wave function, Ψ^0, of retinal can be described by the conjugated valence bond structure shown below:

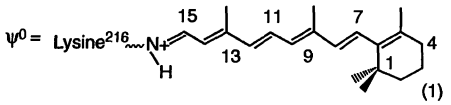

(1)

A COO^- group (such as in Asp^{212} and Asp^{85}) near the N atom of the protonated Schiff base (PSB) will stabilize this structure and thus insure that the C13–C14 bond is a double bond in the ground state. This increases the barrier to the dark (thermal) isomerization process around the C13–C14 bond.

The excited electronic state, Ψ^*, is given by:

$$\Psi^* = \Sigma a_i \psi_i \qquad (2)$$

where ψ_i represent the wave functions for the valence bond resonance structures in which the positive charge resides on carbon 5, 7, 9, 11, 13, or 15. For example, the structure corresponding to ψ_{13} is given by:

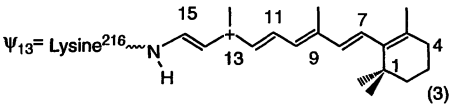

(3)

The values of the coefficients a_i in the sum of Eq. 2 depends on the extent of stabilization of each odd-numbered carbon atom by the negatively charged residues in the retinal cavity. This depends on the shortest distances between the odd-numbered carbon atoms and the O^- of the COO^- groups of Asp^{85} and Asp^{212} as well as on the variations of the dielectric constant within the retinal cavity. The shortest distances (in angstroms) between the O^- of the COO^- group and the Schiff base N atom and the odd-numbered carbon atoms (C15, C13, C11, C9, and C7) of the retinal chain are 4.16, 4.56*, 6.38, 7.99, 9.53, and 10.75* for Asp^{85} and 3.69, 4.16, 5.01, 6.30, 7.73, and 9.422* for Asp^{212} (*28*). From these data, and assuming that the dielectric constant in the retinal cavity is the same everywhere, one may conclude that the COO^- groups on both Asp^{85} and Asp^{212} stabilize the positive charge on the nitrogen of the PSB in the ground state and on the other odd-numbered carbon atoms on the retinal chain in the decreasing order of C15, C13, C11, C9, and C7 in the excited state. Therefore, the double bond charac-

Table 1. The decay parameters of the excited state of retinal in bR and its mutants (*25*).

Sample	Lifetime (ps)	Relative amplitude (fast, slow)	λ_{max} (nm)
wt bR, pH = 4.4–9.6	0.45–0.55	1.0, 0	568
D85N, pH = 4.4–5.8	2.0, 10	0.35, 0.65	604
R82Q, pH = 4.4	2.0, 7.0	0.5, 0.5	596
D212N, pH = 5	2.0, 6.0	0.6, 0.4	566
D212N, pH = 10	2.0	1.0, 0.0	580
R82Q, pH = 9.6	0.6, 5.0*	0.9, 0.1*	556
D115N, pH = 5.8	0.5	1.0, 0	566
Y185F, pH = 5.8	0.55, 5.0*	0.9, 0.1*	578

*Because of the weak signal in the decay curves at long times (see Fig. 1E), these numbers are relatively uncertain.

ter in the excited state (and thus the photoisomerization barrier) is expected to be least around C15–N bond followed by C13–C14 and then C11–C12 and so forth. Because no isomerization occurs around the N–C15 bond, one might conclude that either the geometry of the water molecules around the Schiff base shields the positive charge on C15 in the excited state or else that the isomerization around this bond is sterically hindered because of its closeness to the Lys side chain. Because the stabilization of the positive charge on C13 is more than that on the other odd-numbered carbon atoms in the excited state, the photoisomerization barrier will be least around the C13–C14 bond. This might thus explain the observed selectivity of the photoisomerization process in wt bR.

According to the above model, the selectivity of photoisomerization could be changed if the value of the dielectric constant within the retinal cavity or the shortest distance between the O^- of Asp^{85} or Asp^{212} and odd-numbered carbon atoms of the retinal is changed. Thus the photoisomerization in the mutants or in the retinal analogs could allow isomerization around other bonds as well (*29*). Furthermore, it is possible that in rhodopsin, the stabilization of the positive charge on the retinal chain could be more if it is on C11 than the other odd-numbered carbon atoms of the 11-*cis* retinal in the excited state, allowing for a rapid 11-*cis* to *all-trans* photoisomerization in this system.

The above simple model can also explain the protein catalysis of the dark adaptation process (which involves the thermal isomerization of a fraction of the *all-trans* retinal to the 13-*cis* retinal in the dark) in acid blue bR (*30*) as well as in R82A (*31*) and D85N mutants. Because of the orthogonality of the ground (Ψ^0) and the excited-state (Ψ^*) wave functions, the more the C13–C14 double bond character in the excited state (leading to slow photoisomerization), the less would be the C13–C14 double bond character in the ground state (allowing for more rapid dark isomerization). This analysis leads to the simple rule that in charge stabilization catalysis, perturbations that catalyze the dark (thermal) isomerization around a certain bond will slow down the photoisomerization around the same bond. In acid blue, D85N and R82A, the removal of the negative charge at Asp^{85} position leads to less stabilization of the positive charge on C13 in the excited state and on the Schiff base nitrogen in the ground state. Both the double-bond character in the ground state and the contribution of ψ_{13} to the excited-state wave function decrease as compared to that in wt bR. This can thus account for the observed reduced rate of photoisomerization and the catalysis of the dark adaptation process observed in these systems.

The above results and conclusions suggest that the stabilization effect of the positive charge on C13 in the excited state and on the Schiff base nitrogen in the ground state of the retinal by COO^- groups of Asp^{85} and Asp^{212} catalyze the retinal photoisomerization and reduce the rate of the thermal isomerization (dark adaptation) around the C13–C14 bond in bR. Thus the location of the negative charges and the variation in the value of the dielectric constant within the retinal pocket could control both the selectivity and the rate of the retinal isomerization in the primary photoprocess as well as in the thermal process during the photocycle of the bR photosynthetic system.

REFERENCES AND NOTES

1. D. Oesterhelt and W. Stoeckenius, *Nature* **233**, 149 (1971).
2. E. Racker and W. Stoeckenius, *J. Biol. Chem.* **249**, 662 (1974).
3. For reviews, see R. R. Birge, *Annu. Rev. Biophys. Bioeng.* **10**, 315 (1981); R. H. Callender and B. Honig, *ibid.* **6**, 33 (1977); J. K. Lanyi, in *Bioenergetics*, L. Ernster, Ed. (Elsevier, Amsterdam, 1984), pp. 315–350; *J. Bioenerg. Biomembr.* **24**, 169 (1992); R. Mathies, *Methods Enzymol.* **88**, 633 (1982).
4. D. Oesterhelt, C. Brauchle, N. Hampp, *Q. Rev. Biophys.* **24**, 425 (1991); R. R. Birge, *Annu. Rev. Phys. Chem.* **41**, 683 (1990), and references therein; N. Hampp, C. Brauchle, D. Oesterhelt, *SPIE J.* **1125**, 2 (1989).
5. T. Miyasaka, K. Koyama, I. Itoh, *Science* **255**, 342 (1992).
6. M. P. Heyn, J. Westerhausen, I. Wallat, F. Seiff, *Proc. Natl. Acad. Sci. U.S.A.* **85**, 2146 (1988).
7. T. Hauss, S. Grzesiek, H. Otto, J. Westerhausen, M. P. Heyn, *Biochemistry* **29**, 4904 (1990).
8. S. W. Lin and R. A. Mathies, *Biophys. J.* **56**, 653 (1989).
9. N. R. Hackett, L. J. Stern, B. H. Chao, K. A. Kronis, H. G. Khorana, *J. Biol. Chem.* **269**, 9277 (1987); T. Mogi, L. J. Stern, N. R. Hackett, H. G. Khorana, *Proc. Natl. Acad. Sci. U.S.A.* **84**, 5595 (1987); T. Mogi, L. J. Stern, T. Marti, B. H. Chao, H. G. Khorana, *ibid.* **85**, 4148 (1988). For a review, see H. G. Khorana, *J. Biol. Chem.* **263**, 7439 (1988).
10. K. Gerwert, B. Hess, J. Soppa, D. Oesterhelt, *Proc. Natl. Acad. Sci. U.S.A.* **86**, 4943 (1989); M. Engelhard, K. Gerwert, B. Hess, W. Kreutz, F. Siebert, *Biochemistry* **24**, 400 (1985); L. Eisenstein *et al.*, *J. Am. Chem. Soc.* **109**, 6860 (1987).
11. M. S. Braiman *et al.*, *Biochemistry* **27**, 8516 (1988).
12. R. Henderson *et al.*, *J. Mol. Biol.* **213**, 899 (1990).
13. H. Otto *et al.*, *Proc. Natl. Acad. Sci. U.S.A.* **87**, 1018 (1990); S. Subramanianm, T. Marti, H. G. Khorana, *ibid.*, p. 1013.
14. See the review by R. A. Mathies, S. W. Lin, J. B. Ames, W. T. Pollard, *Annu. Rev. Biophys. Biophys. Chem.* **20**, 491 (1991).
15. R. R. Birge, L. A. Findsen, B. M. Pierce, *J. Am. Chem. Soc.* **109**, 5041 (1987); also see the review by R. R. Birge, *Biochim. Biophys. Acta* **1016**, 293 (1990); S. P. A. Foder *et al.*, *Biochemistry* **27**, 7097 (1988); K. Shulten and P. Tavan, *Nature* **272**, 85 (1978); F. Zhou, A. Windemuth, K. Shulten, *Biochemistry* **32**, 2291 (1993).
16. A. Warshel, *Proc. Natl. Acad. Sci. U.S.A.* **75**, 2558 (1978); A. Warshel and M. Ottolenghi, *Photochem. Photobiol.* **30**, 291 (1979).
17. M. L. Applebury, K. S. Peters, P. M. Rentzepis, *Biophys. J.* **23**, 375 (1978); M. C. Nuss, W. Zinth, W. Kaiser, E. Kolling, D. Oesterhelt, *Chem. Phys. Lett.* **117**, 1 (1985); H. Polland *et al.*, *Biophys. J.* **49**, 651 (1986); J. Dobler, W. Zinth, W. Kaiser, D. Oesterhelt, *Chem. Phys. Lett.* **144**, 215 (1988).
18. R. A. Mathies, C. H. Brito Cruz, W. T. Pollard, C. V. Shank, *Science* **240**, 777 (1988).
19. J. W. Petrich, J. Bretton, J. L. Martin, A. Antonetti, *Chem. Phys. Lett.* **137**, 369 (1987).
20. J. Terner, T. G. Spiro, M. Nagumo, M. F. Nicol, M. A. El-Sayed, *J. Am. Chem. Soc.* **102**, 3238 (1980); J. Terner and M. A. El-Sayed, *Acc. Chem. Res.* **18**, 331 (1985).
21. R. van den Berg, D. J. Jang, H. C. Bitting, M. A. El-Sayed, *Biophys. J.* **58**, 135 (1990); S. J. Doig, P. J. Reid, R. A. Mathies, *J. Phys. Chem.* **95**, 6372 (1991).
22. Briefly, the laser system consisted of a commercial Coherent Satori dye laser pumped by an Antares mode-locked YAG laser. The output of the dye laser was amplified by a regenerative amplifier (Quantel, RGA 60) in a dye amplifier (Quantel, PTA 60) at 10 Hz. The amplified dye laser beam (at 610 nm with an energy of 800 to 1200 μJ per pulse and a 400-fs pulse width full-width at half-maximum) was split into two beams. One was used as the pump beam, and the other was focused into a 5-cm D_2O cell to generate the white light continuum, a portion of which was used to determine the transient absorption. The selected portion of the white light continuum centered at 489 nm with a 10-nm bandwidth was split into a reference beam and a probe beam which had a 300-ps delay. All three beams (pump, probe, and reference) were crossed inside the sample cell, which was translated vertically at a speed of 2 mm/min to reduce accumulation of long-lived photoproducts. The diameters of the laser beams were ~2 mm. The energy of the pump beam was ~20 to 100 μJ and that of the probe and reference was <0.5 μJ. The differential intensity of the probe and reference laser beams was amplified and then averaged by a Box Car integrator, from which the signal was digitized and stored in a computer. The decays obtained for wt bR and the deionized blue bR in our laboratory resemble closely those previously reported by two different laboratories, suggesting that our methodology does not introduce any spurious laser secondary effects.
23. B. Ni, M. Chang, A. Duschl, J. K. Lanyi, R. Needleman, *Gene* **90**, 169 (1990).
24. R. Needleman *et al.*, *J. Biol. Chem.* **266**, 11478 (1991).
25. Abbreviations for the amino acid residues are: A, Ala; C, Cys; D, Asp; E, Glu; F, Phe; G, Gly; H, His; I, Ile; K, Lys; L, Leu; M, Met; N, Asn; P, Pro; Q, Gln; R, Arg; S, Ser; T, Thr; V, Val; W, Trp; and Y, Tyr.
26. T. Kobayashi, M. Terauchi, T. Kouyama, M. Yoshizawa, M. Taiji, *SPIE J.* **1403**, 407 (1990); T. Kobayashi *et al.*, private communication.
27. L. S. Brown, L. Bonet, R. Needleman, J. K. Lanyi, *Biophys. J.*, in press.
28. Numbers without * are kindly provided to us by R. Henderson from his most recently refined protein structure. Numbers with * are obtained from (*12*).
29. U. C. Fischer, P. Towner, D. Oesterhelt, *Photochem. Photobiol.* **33**, 529 (1981); A. Maeda, T. Iwasa, T. Yoshizawa, *Biochemistry* **19**, 3825 (1980).
30. M. K. Mathew, P. Scherrer, W. Sperling, W. Stoeckenius, *Biophys. J.* **49**, 211a (1986).
31. S. Balashov *et al.*, *ibid.* **64**, A212 (1993).

32. We thank the Department of Energy, Office of Basic Energy Sciences (under grants DE-FG03-88ER-13828 at UCLA and DE-FGOER 13525 at UCI) for financial support.

27 April 1993; accepted 18 June 1993